Enhanced Detection of Diabetic Retinopathy from Fundus Images Using Novel Computing Techniques

K. Aldrin Karunaharan[1], K. Abdul Hameed[2]
[1,2]International Maritime College Oman.
[1]aldrin@imco.edu.om, [2]abdul-hameed@imco.edu.om

Abstract

Diabetic retinopathy is a serious eye condition that can cause blindness and visual loss. Diabetic retinopathy is a complication in blood sugar levels that affects the fundus of the eye. We have devised an approach that is based on the classification of probable diseases such as hemorrhage and exudates, followed by feature extraction from the pixel level result and a machine learning method to predict the severity of diabetic retinopathy. Anatomical structures in retinal pictures for instance blood vessels, exudates, and micro aneurysms are segmented, and images are identified as standard or DR images using characteristics extracted from these structures and the Gray Level Co-occurrence Matrix in our research (GLCM). The Support Vector Machine classifier's issue area is these extracted candidates. The Support Vector Machine classifier sorts the images to identify whether the candidate extraction conclusions are microaneurysms or not. The algorithms have been simulated, and the results have been presented. The classifier employed is the Support Vector Machine (SVM), which has a 96 percent accuracy rate.

Keywords: Diabetic Retinopathy, Fundus Photographs, Automated Detection, Blood Vessel Area, Hemorrhage, Exudate.

DOI: 10.47750/pnr.2022.13.S03.056

INTRODUCTION

Diabetes causes diabetic retinopathy, which is an eye disorder. It's a medical disorder in which diabetic persons' eyes build up anomalies because of fluid leaks from blood vessels in the light-susceptible tissue at the back of the eyeball (retina). Ophthalmologists employ color retinal images of a patient taken with a digital fundus camera to make the diagnosis. Diabetic retinopathy is distinguished by traits for example blood vessel section, discharges, internal bleeding, micro-aneurysms, and surface. Multiple approaches exist to diagnose Diabetic Retinopathy (DR). An ocular appearance of diabetes affects more than 75 percent of individuals with long-term diabetes. It is the most important cause of blindness in the people 20-64 age range. According to studies, it accounts for about 5% of all cases of loss of sight. Rendering to the World Health Organization, 347 million people worldwide have diabetes, with 40-45 percent of them at some phase of the condition. Angiogram is obtained by professionals in ophthalmology clinics in the case of diabetic retinopathy and is minimally invasive, posing a risk of side effects to the patient. The National Eye Institute has developed a reliable classification system for DR patients (which are the classes that our classifier predicts). There are four severity classes: non-proliferative DR (NPDR), proliferative DR (PDR), and proliferative DR (PDR). A sequence of four steps characterizes the severity scales.

a. Mild NPDR - Micro-aneurysm lesions, small patches of balloon like ballooning in the retinal blood vessels.
b. Moderate NPDR -Swelling and dilation of blood vessels, widespread micro-aneurysm, retinal hemorrhage.
c. Severe NPDR - Abnormal growth factor secretion is caused by a variety of abnormalities, including massive blot hemorrhages, cotton wool patches, and blocked blood vessels.
d. PDR - Growth factors cause the formation of new blood vessels on the retina's surface.

(a) Normal eye (b) Mild DR eye (c) Moderate DR Eye (d) Severe DR (e) Proliferative DR Eye

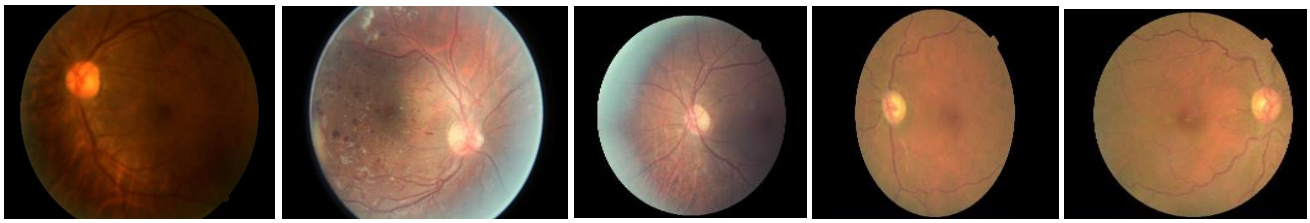

Fig. 1; Classes of DR affected Eyes

The ailment of the vascular composition of human the eye is a crucial distinguishing component in ophthalmology. Retinopathy of sugar patients can be detected by viewing the distinct anatomic features like macula fovea and optical veins which are the evidence of masochist variations. Diabatic retinopathy is depicted by the focal wretchedness of the optical nerve, loss of nerve tissue, and the irregular shape of optic nerve.

Micro red particles in the minor sheets of the retina are the most basic sign of retinopathy. When they are small, they are called microaneurysms, and when their intensity within the retina varies, they are called hemorrhages. This is due to the seepage of blood vessels in the retina, and it indicates moderate retinopathy. When macula edema solidifies within the disc perimeter of the middle of the macula, however, microvascular abnormalities occur, resulting in plasma leaking in the area. This denotes a mild form of retinopathy.

Image acquisition, image pre-processing, optic disc exclusion, feature abstraction, and categorization are the main steps in recognizing an eye disease in diabetes patients. Microscopic fundus pictures are widely used to acquire images. The contrast enhancement of the fundus image is done via an image preprocessing step. Diabetic Retinopathy Detection (DRD) relies heavily on optic disc exclusion because proper removal of the optic disc simplifies the detection method. The structure or quality feature of a retinal image is the focus of feature abstraction. Finally, sorting is completed using a classifier such as a Bayesian classifier, a k-nearest neighbor classifier, or a Support Vector Machine (SVM) classifier. The predicted red color pigment curvilinear form, intensity of the frontier, and differentiation from the background distinguish the blood vessels in the fundus image. Other picture markers, such as the edges of the eye brace and a lack of internal hemorrhage and lacerations, can suggest similar local characteristics as vessels. Blood vessel segmentation is often divided into three types: window-based, classifier-based, and tracking-based. The problem of these approaches is that while waiting for the low-altitude dissection, the comprehensive properties of vessels cannot be applied to the issue. As a result, these attributes can't be used to improve the segmentation, only to evaluate it. Tracking-based techniques use an outline prototype to slowly travel down and slice a vessel.

Edge detection and other window-centered algorithms approximate a pair at each pixel for a specific paradigm in contrast to the pixel's encircling space. The use of classifier-based approaches is divided into two phases. A subordinate procedure creates a dissection of spatially related zones first. As a result, these types of aspiring territories are classified as vessel or non-vessel. In a fundus picture, the Hough transform is used to detect the papilla. Vessel trailing continues iteratively from the papilla, but falters while the reactivity to a single cross-section paired filter falls below a particular threshold. From the beginning, a parallel technique was used to differentiate vessels in coronary arteriograms. One drawback of these approaches is their proclivity for dissolution at wing points, which are difficult to sculpt with a single-dimensional filter. The first stage entails studying about DR disorder and its various grades or stages, each of which is recognized by certain aberrations. The image processing procedures make up the second stage, which is crucial in this field of study. This is because the accuracy of image segmentation decides whether the automated analysis techniques succeed or fail in the end.

LITERATURE SURVEY

Automatic retinal disease screening solutions rely heavily on retinal vascular segmentation algorithms. An overview of strategies for segmenting blood vessels in two-dimensional retinal pictures recorded with a fundus camera is described in the research work by J.U. Nisha. [1] By applying span filtering with a focus on related pixel labeling, these single pixels are deleted. [2] The structure or quality feature of a retinal image is the focus of feature abstraction. Finally, sorting is completed using a classifier such as a Bayesian classifier, a k-nearest neighbor classifier, or a Support Vector Machine (SVM) classifier in the work done by Niabet Med [3] Edge detection and other window-centered algorithms approximate a pair at each pixel for a specific paradigm in contrast to the pixel's encircling space.

The use of classifier-based approaches is divided into two phases.[4] A pixel-based categorization result is the result of the retinal vascular segmentation method. Any pixel can be categorized as a basin or surrounding tissue. [5] Therefore, there are double groupings and two-fold misclassifications to consider. They are: True positive (TP) pixels are those that are classified as vessels in both the ground truth and separated image, while true negative (TN) pixels are those that are categorized as non-liners in both the base truth and segmented image. Image-driven techniques, such as edge-based and region-based approaches; pattern recognition techniques, model-based approaches, tracking-based approaches, and neural network-based approaches are all examples of algorithms for segmenting vessel-like structures in medical images. [6]

However, as Hoover et al. [7] point out, even among professional observers, there is significant inconsistency in vessel identification. The classification criteria in a supervised approach are determined by the ground truth data based on specified features. By applying span filtering with a focus on related pixel labeling, these single pixels are deleted. In the final segmented image, the effect of eliminating these disparate pixels can be observed.[8] Using a one-color photo manipulation application, we identified the particularly apparent ooze out pixels, that were generally light and xanthous patches, picture element by pixel.[9] An erosion procedure detected by a dilation procedure can be regarded as morphological opening. [10] The pixel-level assessment was made by comparing each pixel of the dataset's classification result to precisely labeled ground truth to see if it had exudates.[11]. R. Priya, P. Aruna, SVM and Neural Network based Diagnosis of Diabetic Retinopathy. Automated diagnosis system of diabetic retinopathy have been accomplished by utilizing a set of 250 images which is a mixture of normal, NPDR and PDR affected images.[12] The effectiveness of the feature classification was assessed quantitatively by pixel-by-pixel comparisons of the extracted images with ophthalmologists' hand-drawn ground-truth images. [13]

PREPROCESSING & PROPOSED SYSTEM

The use of image pre-processing for better visualization can significantly improve the consistency of an optical examination. As described in earlier, the recommended system is a DR labelling system that is intended to deal with the three phases of processing. The data mining techniques are included in the third step. Several filter techniques that deepen or reduce particular image elements allow for a more leisurely or speedier evaluation. A geomorphological strainer is used to perform pre-processing in this operation. In pictures, the median pixel quantity within the specified diameter is observed by the median filter. It gets rid of anything that is too bright or too dark. Because median filters do not rely on values that are significantly different from average values in the area, they are particularly effective at removing salt and pepper and impulse noise while keeping image features.

In a similar way as linear filters, median filters work in successive image windows. It arranges all of the pixels in an escalating order to find the central one. Dilation and erosion are often used in pre-processing retinal and fundus images in a variety of ways. To facilitate segmentation of exudates and blood vessels, a picture may be subjected to dilations and attritions sequences. When these two criteria are combined, morphological image inequality and morphological image termination result. An effective thresholding method is required due to the improved vessel segments in the morphological filter rejoinder image.

Peak threshold is calculated by considering the spatial allocations of gray concentrations that are accumulated in the co-occurrence matrix. As a result, it's clear that the threshold image contains micro dissimilar pixels. A screen image is generated for every single figure to guarantee that just the region of the view surrounding the variables is deemed throughout image dealing and assessment. It is used to eliminate any remnants that appear outside of the area of interest.

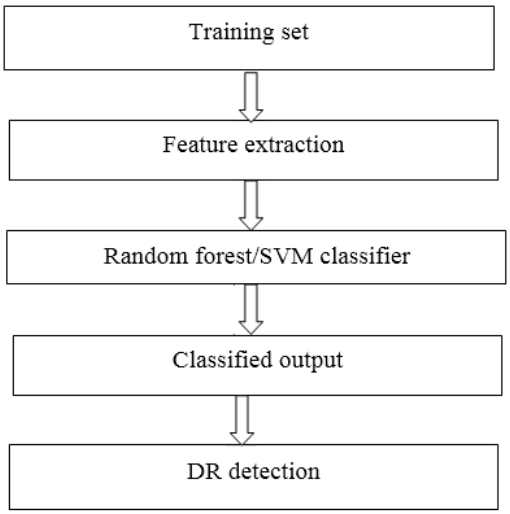

Fig. 2; Proposed Scheme of DR Detection

During eye fundus imaging, the proposed a procedure that diagnoses DR disease. The diabetic retinopathy is identified spontaneously by evaluating the RGB image. Furthermore, the intensity of disease seriousness is reviewed. The dataset is categorized in this system. Normal and abnormal are separated into two categories. Furthermore, the extraordinary retinal pictures are classified into three categories: mild, severe, moderate, and severe.

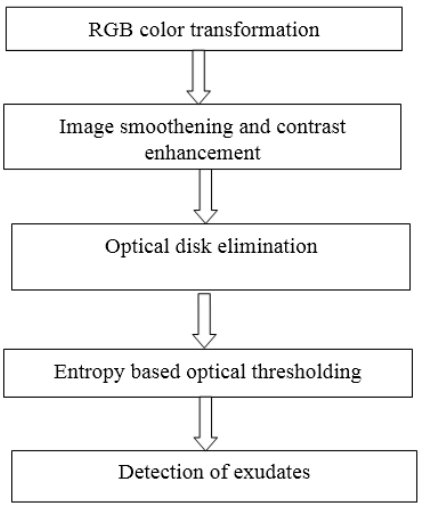

Fig. 3; Scheme for Exudates Detection

SEGMENTATION OF EXUDATES

The optic disc is usually the largest portion and can be easily detected. However, there may be some portions in the picture

that are greater than the optical circle in some instances, such as when there are enormous exudates in the image. Because the optic disc is circular in shape, the region selection technique for the optic disc must be tailored to the largest of the circularly shaped regions. The quantity of efficiency, M, as stated by the subsequent equivalence (1), determines the circularity of the form of the region:

$$M = 4\pi \left(\frac{Area}{Perimeter^{2}}\right) \quad (1)$$

where neighborhood represents the quantity of picture element in the territory and boundary denotes the complete amount of pixels across each region's border.

To guarantee that all picture element in the visual record region are contained, the selected result (biggest among circular forms), OP5, was dilated with a binary dilation operator α in equation (2). This stage makes use of a smooth disc-formed structural component (B2) with a set circle of six.

$$OP_{seg} = \alpha^{B2}(OP5) \quad (2)$$

Using the prior output, the entire optic recording section in the initial image was cloaked out. High contrast vessels, like the previous phases, could be excluded first by a close down operative, which is characterized by P1 in our Eq (3). The previous result was then subjected to a local variation operator, Eq. (3), to produce a universal aberration image that depicts the central portrayal of the narrowly scattered constellation of exudates. The consequent image is shown in fig 3.

$$P_2 = \frac{1}{N-1} \sum (P_1(i) - \mu P_1(x))^2 \quad (3)$$

where x is a set of all pixels in a sub-window), N is a number of pixels and $\mu P_1(x)$ is the mean value of $P_1(i)$. A window size of 6 × 6 was utilized in this phase.

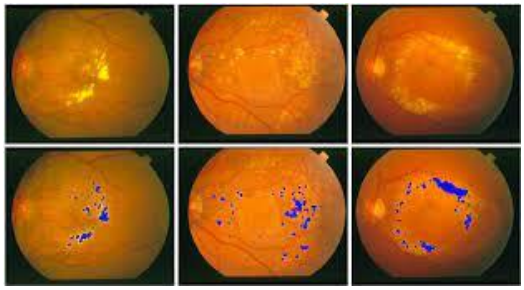

Fig. 4; Exudate Detection

Using the Otsu technique, the generated impression was brined at repeatedly grey concentrations to exclude all places with low local variation. A double dilation operative was used with a smooth disc-sculpted sculpting component with a fixed range to ensure that all of the nearby pixels of the cusped score were also included in the aspirant region, as shown in Eq (4).

$$P_3 = \alpha^{(B_3)} (T\alpha_3(P_2)) \quad (4)$$

Because the candidate zone for denoting transudes would not be limited to their bounds, the roofed neighborhood was flooded. The picture is embodied by P4, as well as the formerly detected optic disc section was dilated before being used to remove the optic disc as of the directly above subsequent flood packed image (P4), Eq. (5). To accomplish this, a double stretching operative with a smooth disc-fashioned configuring component with a static range of (B4) is used.

$$P_5 = P_4 - \alpha^{(B_4)} (OP_{seg}) \quad (5)$$

It was then morphologically reconstructed on the original intensity image using a dilation operator, identical to the procedure taken during the detection of the optic disc. Applying Eq.(6) to the difference between the original image and the reconstructed image, the finishing outcome is generated by employing a thresholding function at a predetermined grayish degree to the distinction sandwiched between the previous picture(F_1) and the restored image (P_5).

$$E_{Seg} = T_{\alpha 4} (F_1 - P_5) \quad (6)$$

This step's outcome will be sent to be validated. The thresholded result is placed on the original image in Fig. 4. In this experiment, there are a lot of variables to consider. The scope of the organizing component (B1, B2, B3, and B4) used for the expansion function, the window size in the regional variant operative, and the maximum values (1, 2, 3, and 4) are all examples. The Otsu algorithm was used to automatically calculate 2 and 3. In a prior experiment, the parameters B1, B2, B3, B4, monitor scale, 1 and 4 remained controlled and evaluated with the intention of evaluating the technique performance.

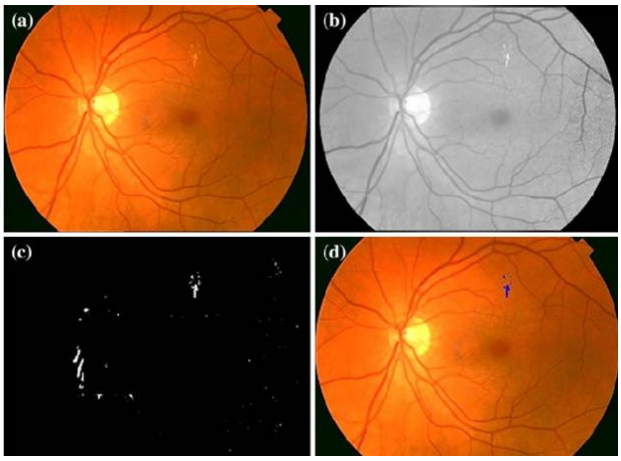

Fig. 5; Hard Exudates Detection

We discovered that adjusting the structuring element size and threshold values had no meaningful effect on the system's performance during the trial with various parameter settings. In this proposed procedure, all parameters are geared up to the assessments that yielded the maximum susceptibility and exactitude in the preceding research. A closing operative deleted the high conflict vessels first. The image was then binarized using thresholding. A macular was defined as the bleakest region in the vicinity of the ophthalmic disc (about 1.5 times the thickness of the optic disc from the position of the optical disc). Thirty three percent of an ophthalmic disc thickness, one optic disc diameter, and two-fold ocular disc diameters were used to create a Macular grid.

An initial draft of a field-reality view was created in order to assist the specialists in producing a ground-truth image. The original image and the original version of the image were then displayed to two professional ophthalmologists. After that, the ophthalmologists made various adjustments, such as combining several unaccounted transude pixels and/or eliminating certain mistaken non-exudate picture element, pending both specialists concurred. There are also several erroneous exudate exposures, which are produced by artefacts that seem like exudates, artefacts from interference in the image possession procedure, transudes near blood arteries, or exudates that occur incredibly feeble. Exudates are mistakenly identified as powerful and elevated juxtapose choroidal plasma veins that emerge and lie in the optic bravado backdrop. Even human specialists are unsure about some equivocal places; therefore, the absence of faint exudates may not have had a significant impact on sensitivity. However, if these low-contrast exudates can be recognized, the algorithm's performance can be enhanced. In order for these kinds of regions to be spotted in the system, we may need to incorporate more specialized features.

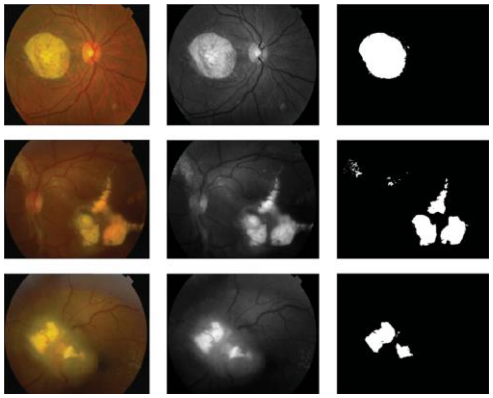

Fig. 6; Original Images [Left] and Detected Images [P1, P2 and P3]

The detection of retinal vessels could potentially be included to help ophthalmologists make optical maser medication assessments. The findings of this research could be used to create an programmed structure for detecting exudates. To improve the system's ability to verify the degree of diabetic retinopathy, microaneurysm and hemorrhage detection could be included. Extending this effort by establishing a scheme to distinguish them will be beneficial.

Feature Selection and Classification

Some critical attributes that were frequently used by eye care consultants to visually separate exudates from other forms of lesions were retrieved from each location and employed as contributions to SVM (support vector machine) in order to further segment the exudates sections from the exudate's entrants. The mean green channel intensity (F1), gray channel intensity (F2), mean hue(F3), standard deviation(F4), and mean gradient magnitude(F5)are the most important characteristics. Depending on which database was utilized, the exudates identification criteria were displayed at two stages: pixel-level and image-level. To create the training vector set, a specific number of pixels (ranging from 50 to 200) were manually selected for each training image. From the eight main features, each pixel formed a feature vector which embodies the input sample feature vector set as representations. Eq[6]

$$x_i = (f_1, f_2, f_3, f_4, f_5) \quad (7)$$

The traditional method of evaluation is to count the number of pixels that were properly classified. A hybrid validation method was applied in this investigation, which requires a low overlap ratio between ground truth and candidates. The aggregate number of white (vessel) pixels in the basin segmented picture is applied to compute the vicinity of plasma vessels. Similarly, the number of white pixels in the exudates and MA images are used to determine the area of exudates and MA, respectively.

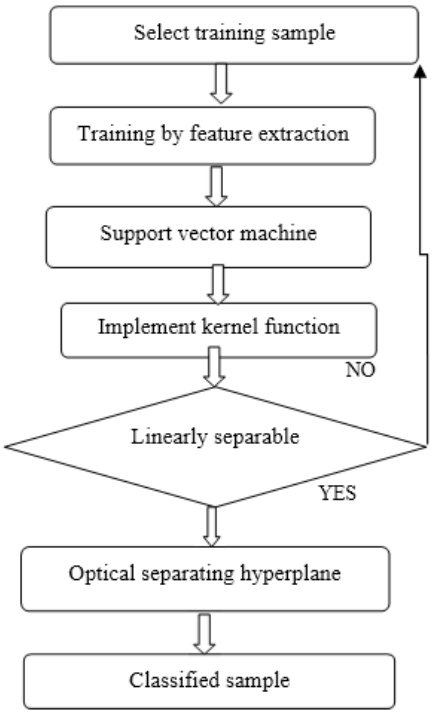

Fig. 7; Scheme for Feature Classification

Nevertheless, this method was ineffective for evaluating exudates segmentation since the contours of exudates do not tally thoroughly between numerous observers' assessments, subsequent in poor exudates segmentation pact.

DR Detection

The proposed approach for DR detection is illustrated in the Fig 7. The feature trajectory for categorization is made up of seven characteristics derived from retinal structure segmentation and texture analysis.

Fig. 8; Fundus Image withe Exudates

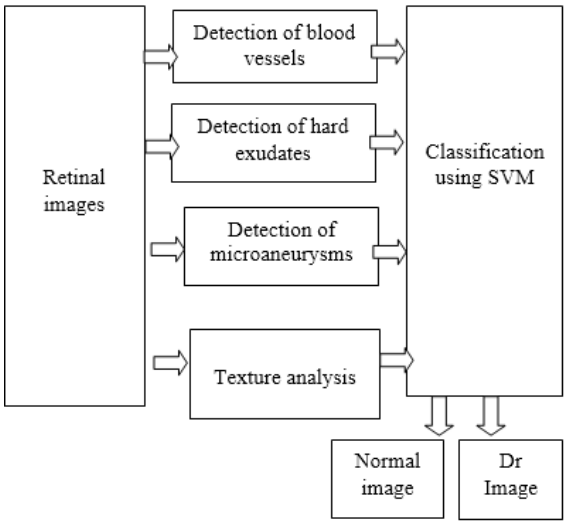

Fig. 9; Scheme for DR Detection

Table 1. Performance Comparison of Automatic DR Detection Systems

Methodology	*No. of test images/No. of exudates*	*SE (%)*	*SP(%)*
Support vector machine SVM	62/17	98.0	84.6
Extreme learning machine ELM	52/8	96.0	89.0
Multilayer perceptron MLV	57/7	100	92.59
Radial basis function RBF	58/9	100	100

Table 1 shows the comparison between various diabetic retinopathy detection techniques in terms of sensitivity and specificity. Approximately 17 exudates are recognized which lead to DR identification as shown in Fig 11. teh classifiers were evaluated based on their mean, standard deviation and F score as shown in fig 10 and performance of the training set used for classification is shown in fig 12. The performance of the classifiers SVM and ELM for MA identification is compared in table 2. It is obvious that when compared to SVM, RBF and the suggested technique using ELM classifier outperforms in terms soft computing parameters such as TP,TN, FP and FN

Table 2. Performance Comparison of Automatic DR Detection Systems in Terms of True Positive

Factors	*SVM*	*ELM (%)*	*RBF*
TP	62/17	98.0	84.6
TN	52/8	96.0	89.0
FP	57/7	100	92.59
FN	58/9	100	100

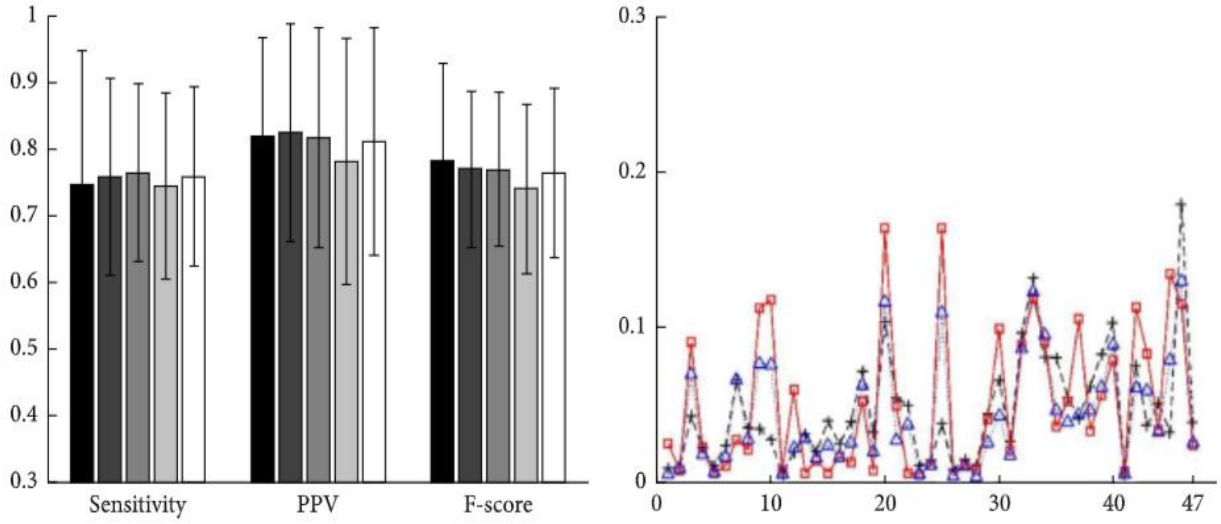

Fig. 10; Evaluation of the Classifier (Overall Mean and Standard Deviation of Sensitivity, PPV, and F-score)

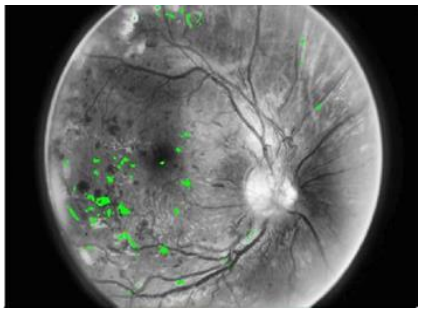

Fig. 11; Detected Exudates[17] Using the Classifier

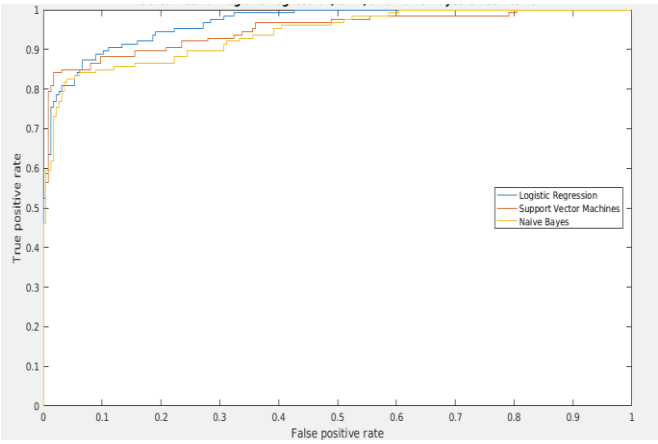

Fig. 12; Performance of the Training Set

The following features are used for the classifier training.

i. Area is he entire number of pixels in a potential region is called its area.
ii. Eccentricity is the ratio of the space between an ellipse's nucleuses to the span of its major axis, and it is 0 for a circular region.
iii. Aspect Ratio is the ratio of the selected region's primary alignment measurement to minor axis span.
iv. Values for the average and universal variation of all green channel pixels in the nominee region.
v. Randomness rate of all pixels in the rectangular territory, including pixels in the candidate region and their neighbors.
vi. The vitality rate of all pixels in the rectangular territory, including those in the nominee region and their neighbors.
vii. The homogeneity value of all pixels in the rectangular region, as well as those in the aspirant region and their neighbour pixels.
viii. The uniformity estimates of all pixels in the square region, including those in the candidate region and their neighbors.

In our approach for DR recognition, we offer the Extreme Learning Machine (ELM), a modern learning procedure for Single Hidden Layer Feedforward Networks (SLFNs) that facilitates in the solution of recession and categorization issues. It can also be utilized to arrive at excellent analytical resolutions, and it learns far quicker than other conventional methods. The input influences and predispositions are chosen at random and do not change during learning iterations. For the hidden neuron layer, you can choose between sine, gaussian, and sigmoidal stimulation tasks, as well as linear activation functions for the output neurons. It's a multi-class classification in which the quantity of yield neurons is proportional to the number of classes. For multi-class categorization (K), the classifiers are normally trained in parallel, with each one trained to distinguish one class from the other K - 1. A one-per-class decomposition is a method of dissecting a general classification problem into dichotomies that is individual of the learning approach used to line up the classifiers. This procedure is a little time consuming and tough. Performance criteria such as Sensitivity (Sen), Specificity (Spec), Positive Predictive Value (PPV), and Accuracy are used to evaluate this proposed study. The equations used to determine these parameters are as follows:

$$\text{Sensitivity \%} = \frac{TP}{(TP+FN)} \times 100$$

$$\text{Specificity \%} = \frac{TN}{(TP+FP)} \times 100$$

$$\text{PPV \%} = \frac{TP}{(TP+FP)} \times 100$$

$$\text{Accuracy \%} = = \frac{TP}{(TP+TN+FP+FN)} \times 100$$

Where,

True Positive (TP): MA areas are those that the classifier correctly classifies.

False Positive (FP): Non-MA regions that the classifier incorrectly classifies as MA regions.

True Negative (TN): Non-MA regions that are accurately categorized by the classifier are called True Negative (TN).

False Negative (FN): MA regions that the classifier incorrectly classifies as non-MA regions.

CONCLUSION

This research work aims to diagnose diabetic retinopathy at an early stage, allowing for a complete cure or a reduction in its progression. The accuracy, sensitivity, specificity, and execution time of this proposed method were assessed, and it was found to be a successful method for automatic early identification of diabetic retinopathy. The suggested support vector machine-based technique has shown promising results in DR detection and exudate recognition, content-based image retrieval, text recognition, biometrics, audio recognition, and regression. When photos were used as input, SVM became famous because it provided better accuracy and precision than other feature classification approaches. We described a method for detecting exudate in a colored retinal image in this article. Preprocessing and picture enhancement, candidate exudate region detection, and feature set building and classification were the three aspects of the suggested system. The bright regions were boosted and segmented with the help of a filter bank and adaptive thresholding, although they had spurious regions that were removed by eliminating the oculus

dexterous pixel. For evaluation purposes, we used sensitivity, specificity, PPV, and accuracy measures. However, the input of automated computing experts is not accepted by the ophthalmologists. SVM and RBF classifiers provided better results based on evaluation parameters. [Table 1].

This work can be expanded in the future to identify exudates, the optic disk, and vascular structures using hybrid techniques to achieve the best results with less complexity and time. The suggested approach offers a low-cost mass screening option for fundus image discrimination to facilitate automated diabetic retinopathy identification. Following fundus image discrimination, diseased images with various lesions can be further categorized based on the intensity range of the lesions.

The darker intensity portion of the dynamic range is occupied by red lesions, whereas the brighter side is occupied by yellow lesions. As a result, these lesions are important in recognizing the presence of DR abnormalities, minimizing ophthalmologists' workload by identifying patients who require early ophthalmic attention. After extensive statistical analysis, 32 prominent features were extracted from a total of 64 features based on the form, intensity, and texture of observed anomalies.

REFERENCES

J.U. Nisha and H.A.R.N, "Splat Feature Classification with Application to Retinal Hemorrhage Detection in Fundus Images", The International Journal of Science & Technology, Vol. 2, No. 4, pp. 338–343, 2014.

R. Sukanya and G. Holi, "Retinal Blood Vessel Segmentation and Optic Disc Detection Using Combination of Spatial Domain Techniques", International Journal of Computer Science Engineering, Vol. 4, No. 3, 102–109, 2015.

Niabet Med 2002;19:105–12. [6] Niemeijer M, van Ginneken B, Staal J, Suttorp-Schulten MS, Abramoff MD. Automatic detection of red lesions in digital color fundus photographs. IEEE Trans Med Imag 2005;24:584–92

C. Heneghan, J. Flynn, M. O'Keefe, M. Cahill, Characterization of changes in blood vessel width and tortuosity in retinopathy of prematurity using image analysis, Medical Image Analysis 6 (2002) 407–429.

A. Haddouche, M. Adel, M. Rasigni, J. Conrath, S. Bourennane, Detection of the foveal avascular zone on retinal angiograms using Markov random fields, Digital Signal Processing 20 (2010) 149–154.

D. Marin, A. Aquino, M.E. Gegundez-Arias, J.M. Bravo, A new supervised method for blood vessel segmentation in retinal images by using gray-level and moment invariants-based features, IEEE Transactions on Medical Imaging 30 (2011) 146–158.

D. Marin, A. Aquino, M.E. Gegundez-Arias, J.M. Bravo, A new supervised method for blood vessel segmentation in retinal images by using gray-level and moment invariants-based features, IEEE Transactions on Medical Imaging 30 (2011) 146–158.

Y.A. Tolias, S.M. Panas, A fuzzy vessel tracking algorithm for retinal images based on fuzzy clustering, IEEE Transactions on Medical Imaging 17 (1998) 263–273.

F. Zana, J.C. Klein, A multimodal registration algorithm of eye fundus images using vessels detection and Hough transform, IEEE Transactions on Medical Imaging 18 (1999) 419–428.

Z. Liang, M.S. Rzeszotarski, L.J. Singerman, J.M. Chokreff, The detection and quantification of retinopathy using digital angiograms, IEEE Transactions on Medical Imaging 13 (1994) 619–626.

SujithKumar S B, Vipula Singh, DzAutomatic Detection of Diabetic Retinopathy in Non-dilated RGB Retinal Fundus Imagesdz, International Journal of Computer Applications, Vol.47, No. 19, June 2012.

Bethanney Janney. J, Sindu Divakaran, Sheeba Abraham, Meera. G and UmaShankar. G, Detection and classification of exudates in retinal image using image processing techniquesdz, Journal of Chemical and Pharmaceutical Sciences, Vol. 8, Issue 3, July-2014.

R. Priya, P. Aruna, DzSVM and Neural Network based Diagnosis of Diabetic Retinopathydz, International Journal of Computer Applications, Vol. 41- No.1, March 2012.

Praveen S Palegar, Dr.K.S. Prabhushetty, Comparative Study of segmentation techniques in Diabetic Retinopathy Detectiondz, International Journal of Advanced Research in Computer Engineering and Technology (IJARCET), Vol. 4, Issue.5, May 2015.

R.F. Mansour, E. Md. Abdelrahim, Amna S. Al-Johani, DzIdentification of Diabetic Retinal Exudates in Digital Color Images Using Support Vector Machinedz, Journal of Intelligent Learning Systems and Applications, August 2015.

Luca Giancardo, Fabrice Meriaudeaub, Thomas P. Karnowskia, Kenneth W., et al "Microaneurysms Detection with the Radon Cliff Operator in Retinal Fundus Images", Medical Imaging, 2010.

S. Jiménez, P. Alemany, F. Nún˜ez Benjumea, C. Serrano, B. Achab, I. Fondón, F. Carral a, C. Sáncheza, "Automatic detection of microaneurysms in color fundus images", 2012.

C. Sinthanayothin, J.F. Boyce, H.L. Cook, T.H.Williamson, Automated localisation of the optic disc, fovea and retinal blood vessels from digital colour fundus images, British Journal of Ophthalmology 83(1999)902–910.

Ibrahim, S., & Koksal, M. E. (2021). Realization of a fourth-order linear time-varying differential system with nonzero initial conditions by cascaded two second-order commutative pairs. Circuits, Systems, and Signal Processing, 40(6), 3107-3123.